PAPER • **OPEN ACCESS**

The synthesis of carbon-based nanomaterials by pulsed laser ablation in water

To cite this article: Entesar A Ganash *et al* 2020 *Mater. Res. Express* **7** 015002

Materials Research Express

PAPER

The synthesis of carbon-based nanomaterials by pulsed laser ablation in water

Entesar A Ganash , Ghaliah A Al-Jabarti and Reem M Altuwirqi

Physics Department, Faculty of Science, King Abdulaziz University, Jeddah, Saudi Arabia

E-mail: eganash@kau.edu.sa

Keywords: carbon-based nanomaterials, pulsed laser ablation, graphene, reduced graphene oxide

OPEN ACCESS

RECEIVED
15 October 2019

REVISED
8 November 2019

ACCEPTED FOR PUBLICATION
13 November 2019

PUBLISHED
25 November 2019

Abstract

Pulsed Laser Ablation in liquid (PLAL) is considered as a robust and simple technique for producing nanoparticles (NPs) using lasers. The carbon-based nanoparticles were fabricated via the PLAL approach by irradiating a graphite target with a pulsed Nd:YAG laser of wavelength 532 nm. The graphite target was immersed in distilled water and irradiated for 10 min. The pulse length, reputation rate, and fluence were 6 ns, 10 Hz, and 0.4 J cm^{-2}, respectively. The structural and physical properties of the synthesized NPs were investigated and analyzed using different characterization methods. For example, Transmission Electron Microscopy (TEM) images revealed diverse carbon nanostructures such as graphene nanosheets, nanospheres, nanospheres in the shape of a necklace, and nanotubes. The spectrum of Energy Dispersive X-Ray spectroscopy (EDX) confirmed successful synthesis of high purity carbon nanostructures. Moreover, the result of X-Ray Diffraction (XRD) Spectroscopy indicated the presence of reduced Graphene Oxide (rGO) with a (002) plane and the absence of Graphene Oxide (GO). The transmission spectrum from Ultraviolet-Visible (UV–vis) analysis showed a strong trough at 266 nm which is attributed to the presence of carbon nanostructures. Furthermore, Fourier-Transform Infrared Spectroscopy (FTIR) analysis demonstrated the vibration bonds related to carbon. The nanostructures produced were semi-stable with little agglomeration as was inferred from the results of the Zeta Potential. Finally, the Dynamic Light Scattering (DLS) analysis supported the TEM results. PLAL technique is proved to be a simple method for producing carbon-based nanomaterials. Moreover, the laser fluence was found to be an important factor which affects greatly the type of nanostructures that could be synthesized during laser ablation.

1. Introduction

After fullerene's discovery, various forms of carbon nanostructure including carbon nanoparticles (CNPs), nanotube, onions, and nanocages were recognized [1]. Carbon-based nanomaterials have attracted great interest in the recent decades due to their unique physical properties (electrical, thermals, optical and mechanical). This opened up the way for many applications in many fields such as physics, chemistry and engineering. Now, carbon nanomaterials are being investigated as active materials in electronic devices, energy storage, energy conversion devices (lithium-ion batteries), solar cells, field emission electron sources, nanometer-sized semiconductor devices, supercapacitors, sensors and lubricant additives [2–8].

The carbon nanostructures were synthesized by several methods such as chemical vapor deposition (CVD), discharge in protection gases and microwave plasma [9]. In the current years, there has been an increasing interest in the pulsed laser ablation in liquid (PLAL) method to fabricate different nanomaterials. PLAL has been used to synthesize different elements nanoparticles (NPs), for example gold [10–12], sliver [13, 14], and copper [15, 16]. In this technique, a laser interacts with the sample under study, which is submerged in a liquid, and a laser induced breakdown occurs. Shock waves are then generated, and the created plasma expands and cools. After that, a cavitation bubble is produced, expands and finally collapse by the liquid. Consequently, NPs are released in the liquid [17]. The main advantage of using PLAL is that it does not require vacuum equipment for

the NPs fabrication, hence, it is a low cost and a simple technique. Moreover, after the particles' fabrication by this method they are easily collected [9]. The properties of nanomaterials synthesized by the laser ablation of solids in liquids depend on two factors: firstly, the laser parameters such as the wavelength, pulse energy, exposure duration and the laser repetition rate. Secondly, the material parameters namely bulk target, solvent, solutes, and the system temperature and pressure [18].

In 1992, Ogale *et al* [19] synthesized diamond particulates with sizes ranging from 5 to 20 μm by using the pulsed ruby laser ablation of pyrolytic graphite surface submerged in benzene. Also, in 1993, Fojtik and coworkers [20] used the ruby laser irradiation of graphite microparticles suspended in a toluene liquid in fabricating carbon clusters. Following these pioneering studies, a considerable amount of literature has been published on PLAL. Moreover, CNPs were fabricated using PLAL using infrared (IR) laser Nd:YAG with a 1064 nm wavelength on graphite and polycrystalline diamond targets, which were immersed in both liquids: deionized water and isopropanol. Dudek *et al* studied the effect of changing average power in a range 0.18–7.52 W on the size of resulted particles [21]. In addition, the influence of liquid temperature on the characteristics of carbon nanostructures produced via PLAL was investigated by Asl [22]. Their results showed an increase of the CNPs and a decrease of the rate of graphene nanosheets with increasing distilled water temperature. Another study investigated the effect of using different liquid media (distilled water, acetone, alcohol, and cetyltrimethylammonium bromide (CTAB)) on the morphology, structure and optical properties of carbon nanostructures prepared via PLAL [23]. Zamiranvari and collaborator [24] found that the concentration level of CTAB as the ablation medium affected the properties of the produced graphene nanosheets fabricated by laser ablation of graphite target. Moreover, the relationship between the laser fluence and the characterization of carbon nanostructures synthesized by laser ablation in liquid nitrogen was considered experimentally by Tabatabaie and Dorranian [25]. They found that a threshold fluence exists for the production of CNPs and when laser fluence was increased more CNPs were produced. On the other hand, with increasing fluence, the amount of graphene nanosheets were reduced.

To the other end of the spectrum, some workers used UV wavelength to produce carbon nanostructures. For example, Luo and collaborator [26] used krypton fluoride (KrF) pulsed laser irradiation (wavelength of 248 nm and a laser fluency of 0.8 J pulse^{-1} cm^{-1}) in ethanol at ambient conditions to produce silicon carbide (SiC) @graphene nanocomposites in a one-step laser irradiation process.

Moreover, some studies reported the fabrication of carbon nanostructures via PLAL method using the second harmonic wavelength of Nd:YAG laser (532 nm) to demonstrate the vital role of laser wavelength on the produced carbon nanostructures. For instance, Tarasenka and colleagues [27] investigated the influence of different liquid medium (water, ethanol and 0.008 m aqueous diethylenetriaminepentaacetic acid (DTPA) solution) on the morphology, structure and optical properties of CNPs fabricated using an unfocused Nd:YAG laser (532 nm) on graphite. Many carbon nanostructures were fabricated by the laser ablation using the 532 nm wavelength such as nanocrystalline diamond [28], graphene sheets [29, 30], CNPs [31] and nanotubes [32].

The purpose of this research is to investigate the effect of laser fluence on the type of carbon-based nanomaterials produced using PLAL technique with the implementation of the second harmonic of Nd:YAG laser (532 nm). Different analytical techniques will be used to describe the synthesized carbon nanomaterials synthesized in this work.

2. Experimental

Prior to running the experiment, all glassware were washed with distilled water followed by acetone and finally cleaned ultrasonically with the distilled water to ensure the absence of any contamination. A Q-switched pulsed Nd:YAG Laser (Quanta Ray, Spectra Physics) operated in its second harmonic wavelength (532 nm) was used to irradiate for 10 min a high purity graphite rod (99.997% purity, Goodfellow), which was polished with a sand paper then washed with distilled water. The graphite target was placed at the bottom of a glass cylindrical container filled with distilled water where its level was about 0.8 mm above the target. A converging lens (Thorlabs LB5284 CaF2 Bi-Convex Lens, f = 50.0 mm, Uncoated) was used for focusing the laser beam on the target surface. A prism (Thorlabs PS704 CaF2 Right-Angle Prism, Uncoated, 25 mm) was used to direct the laser beam to irradiate the sample. Pulses of 6 ns duration with a reputation rate of 10 Hz and energy density of 0.4 J cm^{-2} were applied. A Thorlabs thermal power sensor (S350C, range 0.19–1.1 μm and 10.6 μm, 40 W) attached to a power meter console (Thorlabs PM100D) was used to measure the average power of the pulsed laser beam and assures the stability of the laser power during the experiment. It should be pointed that in order to avoid crater formation on the target, the target was placed on an XY stage and moved constantly and cautiously during the laser ablation allowing the laser beam to hit the target surface at different positions. Furthermore, the experiment was carried out at room temperature. The experimental setup is shown in figure 1.

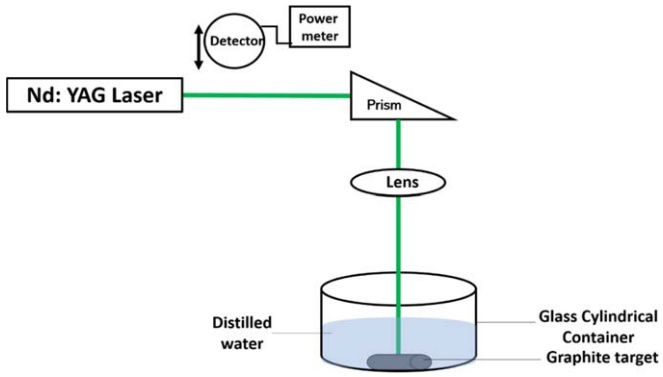

Figure 1. A schematic diagram of the experimental set up for pulsed laser ablation in distilled water.

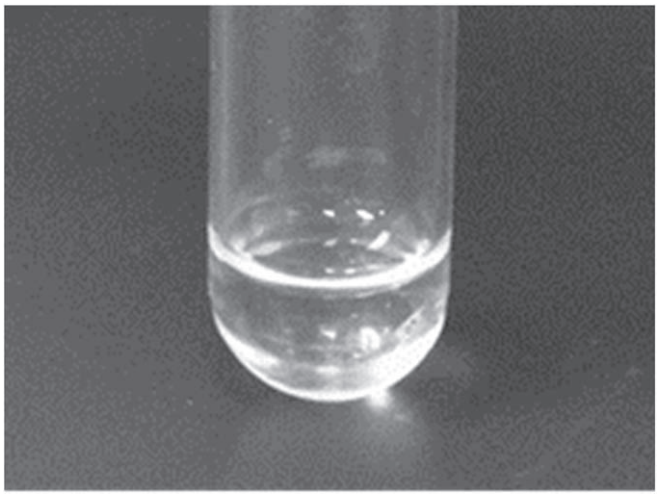

Figure 2. Colloidal solution from PLAL of graphite target in distilled water.

After the completion of the experiment, the colloidal solution containing the nanomaterial was taken to perform the different characterizations. For example, Transmission Electron Microscopy (TEM, Tecnai G20, Super twin, double slit, FEI, Netherlands) images were obtained to investigate the morphology of the produced nanomaterials. In addition, elemental composition of the resulted material was examined using Energy Dispersive x-ray spectroscopy (EDX, Bruker Nano Berlin, Germany). X-Ray Diffraction (XRD) Spectroscopy (Rigaku Ultima_iv, CuK_{α} radiation, $\lambda = 1.54$ Å, operating at 40 Kv and 40 mA, scanning angles in the range 5°–90°, and scanning step of 0.1°) was used to study the structure of the fabricated nanomaterials, Moreover, to analyze the optical properties of the nanomaterials, UV–vis spectrophotometry (Thermo, Genesys 10 S model) was employed. Fourier transform infrared spectroscopy (FTIR, PerkinElmer, Spectrum 100) was used to investigate the chemical bonds of the produced suspension. Finally, the charges on the surface of the produced nanostructures and their size distribution were measured by zeta potential and Dynamic Light Scattering technique (Zeta sizer nano series, Malvern, UK).

3. Results and discussion

3.1. The synthesis of carbon-based nanomaterials

The produced carbon nanostructures suspension is shown in figure 2. In PLAL method, it is suspected that many forms of carbon-based structures will be produced. For example, structures such as fullerene molecules, diamond-like carbons, carbon spheres, and graphene nanosheets can be expected to be in the obtained colloidal solution after laser irradiation. It can be seen from figure 2 that the suspension is colorless which might be an indication of the dominance of graphene sheets in the solution, as they are transparent and colorless. Carbon nanospheres are usually dark gray and tend to make the suspension opaque. Hence, it is assumed that using PLAL in liquid with a fluence of 0.4 J cm^{-2}, that was set in this work, may enhance the production of graphene

sheets in comparison to other carbon-based nanomaterials. This agrees with previous work [25] where it was concluded that increasing the laser fluence results in the production of carbon nanoparticles, while decreasing the fluency increases the production of graphene nanosheets, however, to our knowledge no work was done with fluence as low as 0.4 J cm^{-2}. In this work, several analytical methods were used to investigate the obtained suspension as discussed in the below section.

3.2. Characterization of carbon nanostructures

3.2.1. TEM analysis

The size and morphology of the synthesized carbon nanostructures were studied using TEM. The TEM images showed different carbon-based structures (figures 3(a) and (b)). These included graphene nanosheets, carbon nanotubes and carbon nanospheres. The dominance was for the graphene nanosheets whether in single or multi layers. Looking into the images in more depth, some measurements can be made on the size of the nanostructures found in the colloidal solution. In figure 3(c) graphene nanosheets, carbon nanotubes and carbon nanospheres can be seen. The size of some of the nanosheets were 200 nm, approximately. As for the carbon nanospheres, the diameter was about 45 nm. The measurements of the carbon nanotubes had a length of 140 nm and a diameter of 21 nm. Figure 3(d) illustrates stacked graphene sheets with the inset showing its edges. The multi-layers can be distinguished from its dark color which indicates stacked number of sheets. Another feature that was observed is the formation of a necklace of carbon nanosphere (figure 3(e). Carbon nanospheres with diameters less than 100 nm tend to accrete or form a necklace structure [33]. They are attracted with each other by Van der Waals forces and this leads to agglomerated collections of the carbon nanospheres. There are some factors that yield to the accretion of carbon nanospheres such as extended reaction times and cooling from synthesis to room temperature [34]. These necklaces were not a dominant feature in the colloidal solution. The average diameter of the carbon nanospheres in the necklace formation was 60 ± 11 nm. Figures 3(f), (g) and (h) shows the necklace formation at different magnification along with the particle size distribution.

3.2.2. EDX analysis

Figure 4 shows the EDX spectrum of the synthesized carbon nanostructures. It indicates the presence of only carbon as a primary element and oxygen. This result confirms the successful synthesis of high purity carbon nanostructures. Furthermore, the percentage of oxygen is very low which might indicate the absence of graphene oxide from the sample. This will be further investigated from the XRD analysis in the following subsection.

3.2.3. XRD analysis

Each crystalline material has a distinctive XRD pattern. Hence, XRD patterns are like fingerprints that assist in identifying materials. For this technique, a thin film was prepared from a few drops of the colloidal solution that was deposited on a glass slide and dried at100 °C for 30 min. Figure 5 shows the XRD spectrum of the thin film that was prepared in this work. The XRD pattern of graphite illustrates a strong diffraction peak at $2\theta = 26.6^{\circ}$ which corresponds to the (002) plane and weak peaks at $2\theta = 42.2^{\circ}$ and 44.3° which correspond to the (100) and (101) planes, respectively (JCPDS, Card No. 75-1621). It can be seen from figure 5 that a broad peak is exhibited at $2\theta = 25^{\circ}$. This peak is near the position of the graphite peak of the (002) plane. Since graphite is only stacked layer of graphene, then they would naturally have planes that are similar in their interplanar spacing and thus similar diffraction angles. The broadened peak is attributed to the fact that the stacked graphene layers were not well ordered [35]. The more ordered the stacked graphene layers, the more these layers will resemble graphite and the diffraction peak becomes narrower. Furthermore, since there is a peak at 25° with reasonable width, it indicates that graphene is present in stacked layers form and that they are not monolayers. If graphene monolayers are present in the sample, no peak will be observed [36]. Graphene oxide (GO) has a characteristic peak at $2\theta = 11.4^{\circ}$, which corresponds to the (001) plane [37]. Since no peak at 11.4° was observed in figure 5, this indicates that GO is not present in the sample and that it could have been reduced to form reduced graphene oxide (rGO). The broad peak observed in figure 5 occurs at $2\theta = 25^{\circ}$ and not at $2\theta = 26.6^{\circ}$ as in pure graphite. The shift in the peak can be concluded that oxygen still remains between the graphene layers causing the spacing between the layer to be greater than that in graphite [37]. This agrees with the EDX analysis where there was a low percentage of oxygen in the sample, but it was not eliminated completely.

3.2.4. UV–vis analysis

The UV–vis spectrometer was used to measure the transmission spectrum of the colloidal solution in the 200–1100 nm region (figure 6). Carbon generally exhibits an absorption peak in the range of 180–280 nm [38]. The absorption peak at 266 nm of carbon nanostructures is assigned to the π–π^* transition of C=C bond [39]. It can be seen from figure 6 that a trough at 266 nm is present in the transmission spectrum (corresponding to the

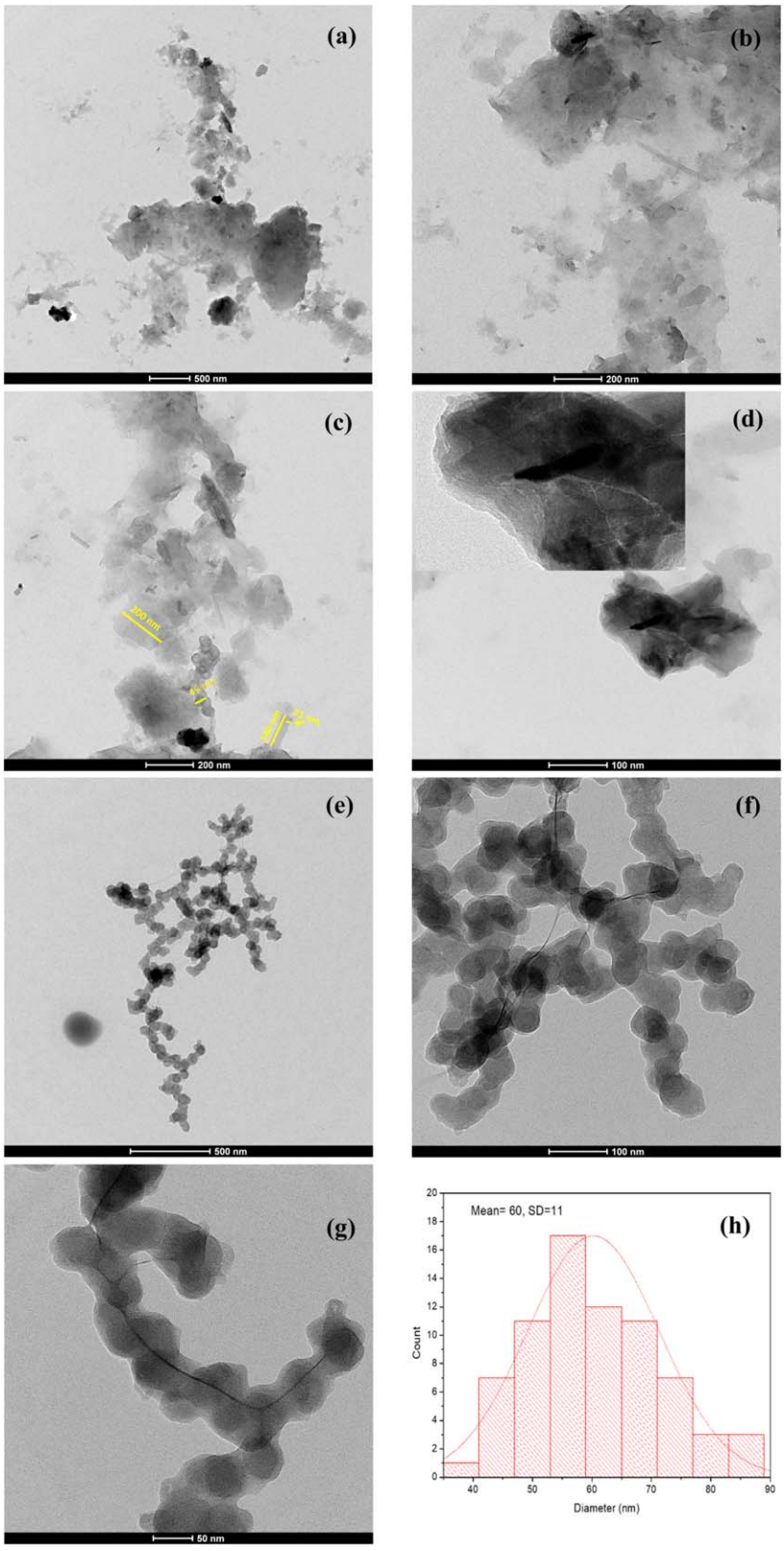

Figure 3. TEM image of carbon nanostructures in the colloidal solution at (a) 500 nm and (b) 200 nm magnifications, (c) carbon nanosheets, nanotubes and nanospheres with measurements, (d) stacked nanosheets (inset: enlarged nanosheets showing the edges), (e) carbon nano-necklace, (f) and (g) magnification of carbon nanospheres in the nano-necklace, and (h) particle size distribution of nanosphere in the nano-necklace.

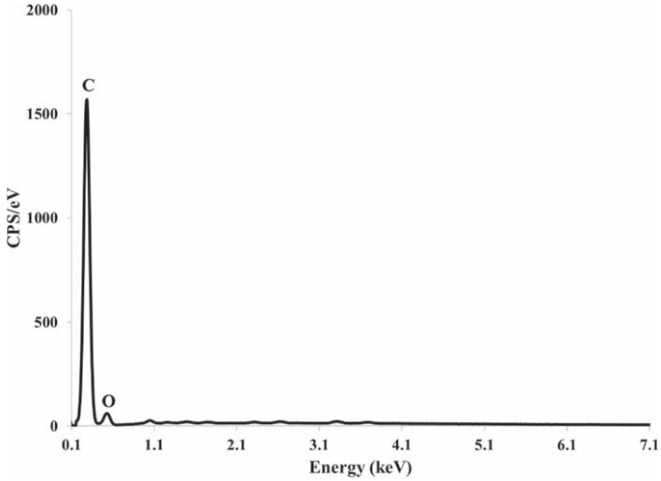

Figure 4. Spectrum from EDX analysis.

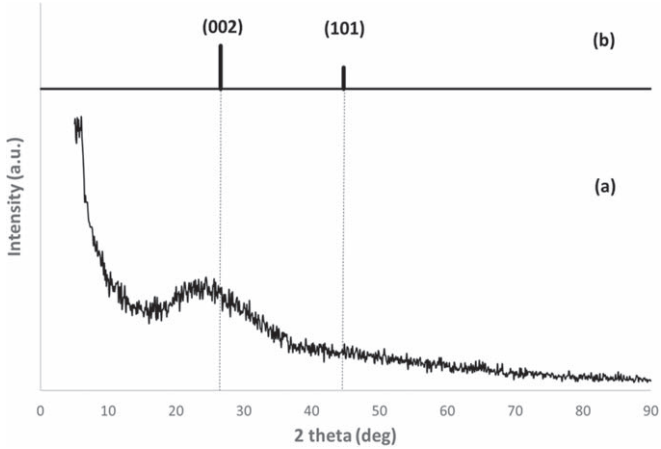

Figure 5. XRD spectrum of (a) the prepared sample, (b) stick pattern of graphite (JCPDS, Card No. 75-1621).

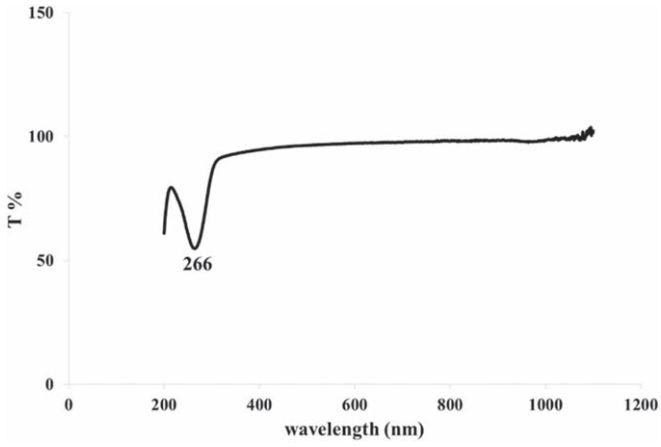

Figure 6. UV–vis transmission spectrum of carbon nanostructures suspension.

absorption peak). Hence, this confirms the presence of carbon nanostructures in the obtained suspension. Since no other troughs are seen in the spectrum, it can be concluded that only carbon particles were found.

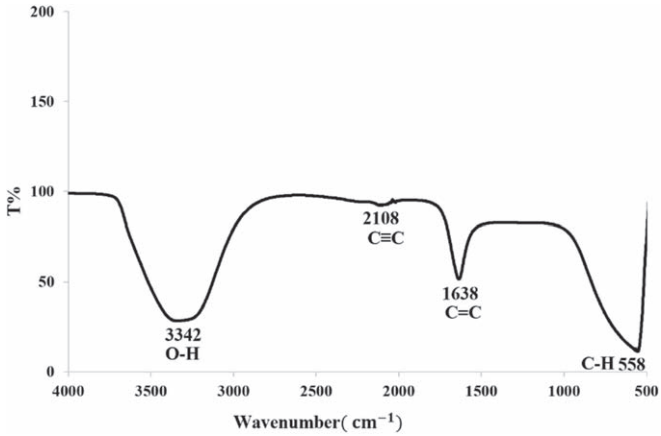

Figure 7. FTIR spectrum of carbon nanostructures suspension.

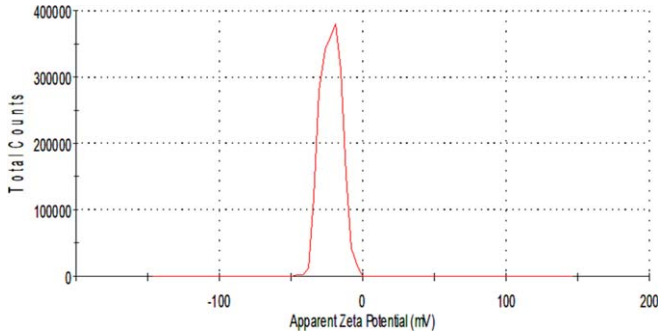

Figure 8. Zeta potential of the prepared sample.

3.2.5. FTIR analysis

The FTIR spectra are usually used to investigate the different chemical bonds of materials. In this work, FTIR spectroscopy was used to analyze the carbon nanostructures solution in the range of 550–4000 cm^{-1}. Four distinct troughs were observed in the FTIR spectrum of the sample. These are 3342, 2108, 1638, and 558 cm^{-1} as seen in figure 7. The trough at 3342 cm^{-1} is related to water O–H stretching vibration mode [40]. Similarly, the trough at 2108 cm^{-1} is attributed to carbon–carbon triple bond (C≡C) [5, 41]. The aromatic C=C vibrations cause the appearance of a trough at around 1638 cm^{-1} [30]. Finally, the trough at 558.92 cm^{-1} is related to C–H bond [42].

3.2.6. Zeta potential analysis

Zeta potential is a physical characterization, which describes the total charge on the surface of nanoparticles [43]. Zeta potential result shows that the carbon nanostructures in our sample have a negative charge of the value −22 mV. This amount of charge results in the existence of repulsion forces between the particles and consequently reduces their agglomeration [44]. Figure 8 shows the zeta potential distribution of our sample.

3.2.7. DLS analysis

To measure the size distribution of the nanoparticles, present in a suspension, the DLS analysis technique is usually used. The results illustrated in figure 9 give information of the size of the nanostructures present in the colloidal solution of the prepared sample. When taking the sample as is without filtering, a single peak in the DLS spectrum appears. This peak indicates a size of 520 nm of the nanostructures in the solution. Since no other peak was present in the spectrum, the solution can be regarded as dominated by these structures that has the size of 520 nm. From the TEM and XRD analysis, it was apparent that the solution is mainly composed of graphene nanosheets that have large lengths. Although carbon nanospheres were observed in the TEM images, there is no indication of their presence in figure 9(a). By using a 100 nm nanometric filter, particles larger than 100 nm can be removed. Figure 9(b) displays the DLS spectrum of the filtered sample. It can be seen that now two peaks appear in this figure. The more intense peak indicates average structure size of 574 nm and compromising 73%

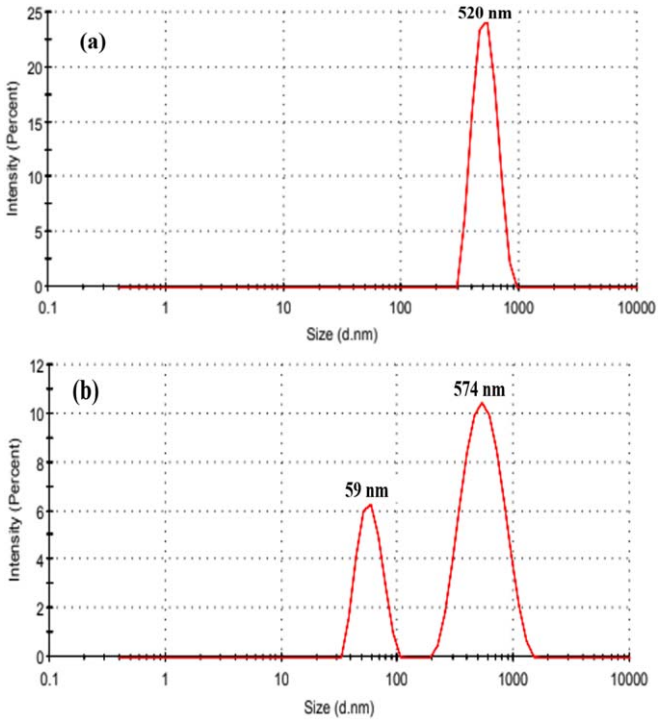

Figure 9. Size distribution of carbon nanostructures determined by DLS (a) without a filter (b) with 100 nm nanometric filter.

of the sample constituents, while the second peak reports particles of an average size of 59 nm with abundance of 27%. This agrees with the observed TEM images where the nanospheres in the necklace had an average size of 60 nm (figure 3(h)) although they were not dominant in the sample. The presence of structures larger than 100 nm even after using the 100 nm nanometric filter might indicate that the graphene sheets were folded.

4. Conclusion

This study has shown that PLAL technique is a successful method for synthesizing carbon-based nanostructures. It was found that the laser fluence is an important factor for determining the carbon nanostructures obtained through PLAL. Reducing the fluence of a 532 nm Nd:YAG laser beam to 0.4 J cm^{-2}, and using it to irradiate a graphite target submerged in distilled water, resulted in the synthesis of rGO nanosheets which constituted, approximately, 73% of the nanostructures in the sample.

Acknowledgments

The authors are thankful to Physics Department, Faculty of Science at King Abdulaziz University, Jeddah, Saudi Arabia for supporting this work.

ORCID iDs

Entesar A Ganash https://orcid.org/0000-0002-8058-4928

References

[1] Chen G X, Hong M H, Chong T C, Elim H I, Ma G H and Ji W 2004 Preparation of carbon nanoparticles with strong optical limiting properties by laser ablation in water *J. Appl. Phys.* **95** 1455–9
[2] Baughman R H, Zakhidov A A and De Heer W A 2002 Carbon nanotubes—the route toward applications *Science* **297** 787–92
[3] De las Casas C and Li W 2012 A review of application of carbon nanotubes for lithium ion battery anode material *J. Power Sources* **208** 74–85
[4] Zhu H, Wei J, Wang K and Wu D 2009 Applications of carbon materials in photovoltaic solar cells *Sol. Energy Mater. Sol. Cells* **93** 1461–70
[5] Yan J, Uddin M, Dickens T and Okoli O 2013 Carbon nanotubes (CNTs) enrich the solar cells *Sol. Energy* **96** 239–52

[6] Notarianni M, Liu J, Vernon K and Motta N 2016 Synthesis and applications of carbon nanomaterials for energy generation and storage *Beilstein J. Nanotechnol.* **7** 149–96
[7] Wang Q and Arash B 2014 A review on applications of carbon nanotubes and graphenes as nano-resonator sensors *Comput. Mater. Sci.* **82** 350–60
[8] Luo T, Chen X C, Li P S, Wang P, Li C C, Cao B Q, Luo J B and Yang S K 2018 Laser irradiation-induced laminated graphene/MoS_2 composites with synergistically improved tribological properties *Nanotechnology* **29** 11
[9] Thongpool V, Asanithi P and Limsuwan P 2012 Synthesis of carbon particles using laser ablation in ethanol *Procedia Engineering* **32** 1054–60
[10] Kim H J, Bang I C and Onoe J 2009 Characteristic stability of bare Au-water nanofluids fabricated by pulsed laser ablation in liquids *Opt. Lasers Eng.* **47** 532–8
[11] Amendola V, Polizzi S and Meneghetti M 2006 Laser ablation synthesis of gold nanoparticles in organic solvents *J. Phys. Chem.* B **110** 7232–7
[12] Amendola V, Rizzi G A, Polizzi S and Meneghetti M 2005 Synthesis of gold nanoparticles by laser ablation in toluene: quenching and recovery of the surface plasmon absorption *J. Phys. Chem.* B **109** 23125–8
[13] Ganeev R A, Baba M, Ryasnyansky A I, Suzuki M and Kuroda H 2004 Characterization of optical and nonlinear optical properties of silver nanoparticles prepared by laser ablation in various liquids *Opt. Commun.* **240** 437–48
[14] Valverde-Alva M A, García-Fernández T, Villagrán-Muniz M, Sánchez-Aké C, Castañeda-Guzmán R, Esparza-Alegría E, Sánchez-Valdés C F, Llamazares J L S and Herrera C E M 2015 Synthesis of silver nanoparticles by laser ablation in ethanol: a pulsed photoacoustic study *Appl. Surf. Sci.* **355** 341–9
[15] Moniri S, Ghoranneviss M, Hantehzadeh M R and Asadabad M A 2017 Synthesis and optical characterization of copper nanoparticles prepared by laser ablation *Bull. Mat. Sci.* **40** 37–43
[16] Muniz-Miranda M, Gellini C, Simonelli A, Tiberi M, Giammanco F and Giorgetti E 2013 Characterization of Copper nanoparticles obtained by laser ablation in liquids *Appl. Phys. A-Mater. Sci. Process.* **110** 829–33
[17] Dell'Aglio M, Gaudiuso R, De Pascale O and De Giacomo A 2015 Mechanisms and processes of pulsed laser ablation in liquids during nanoparticle production *Appl. Surf. Sci.* **348** 4–9
[18] Amendola V and Meneghetti M 2009 Laser ablation synthesis in solution and size manipulation of noble metal nanoparticles *Phys. Chem. Chem. Phys.* **11** 3805–21
[19] Ogale S B, Malshe A P, Kanetkar S M and Kshirsagar S T 1992 Formation of diamond particulates by pulsed ruby-laser irradiation of graphite immersed in benzene *Solid State Commun.* **84** 371–3
[20] Fojtik A and Henglein A 1993 Laser ablation of films and suspended particles in a solvent - formation of cluster and colloid solutions *Ber. Bunsen—Ges. Phys. Chem. Chem. Phys.* **97** 252–4 Accession Number: WOS:A1993KW56500016
[21] Dudek M, Rosowski A, Koperkiewicz A, Grobelny J, Wach R, Sharp M, French P, Janasz L and Kozanecki M 2017 Carbon nanoparticles fabricated by infrared laser ablation of graphite and polycrystalline diamond targets *Phys. Status Solidi* (A) **214** 1–8
[22] Asl P M and Dorranian D 2016 Effect of liquid medium temperature on the production rate and quality of graphene nanosheets produced by laser ablation *Opt. Quantum Electron.* **48** 12
[23] Sadeghi H and Dorranian D 2016 Influence of size and morphology on the optical properties of carbon nanostructures *J. Theor. Appl. Phys.* **10** 7–13
[24] Zamiranvari A, Solati E and Dorranian D 2017 Effect of CTAB concentration on the properties of graphene nanosheet produced by laser ablation *Opt. Laser Technol.* **97** 209–18
[25] Tabatabaie N and Dorranian D 2016 Effect of fluence on carbon nanostructures produced by laser ablation in liquid nitrogen *Appl. Phys. A-Mater. Sci. Process.* **122** 9
[26] Luo T, Chen X, Wang L, Wang P, Li C, Iqbal S and Cao B 2018 Ultrafast synthesis of SiC@graphene nanocomposites by one-step laser induced fragmentation and decomposition *Ceram. Int.* **44** 19028–32
[27] Tarasenka N, Stupak A, Tarasenko N, Chakrabarti S and Mariotti D 2017 Structure and optical properties of carbon nanoparticles generated by laser treatment of graphite in liquids *Chem. Phys. Chem* **18** 1074–83
[28] Yang L, May P W, Yin L, Smith J A and Rosser K N 2007 Growth of diamond nanocrystals by pulsed laser ablation of graphite in liquid *Diam. Relat. Mat.* **16** 725–9
[29] Qian M, Zhou Y S, Gao Y, Feng T, Sun Z, Jiang L and Lu Y F 2012 Production of few-layer graphene through liquid-phase pulsed laser exfoliation of highly ordered pyrolytic graphite *Appl. Surf. Sci.* **258** 9092–5
[30] Vaghri E and Dorranian D 2016 Effect of ablation environment on the characteristics of graphene nanosheets produced by laser ablation *Stud. Univ. Babes-Bolyai Chem.* **61** 277–84 Accession Number: WOS:000393578800023
[31] Chen G X, Hong M H, Tan L S, Chong T C, Elim H I, Chen W Z and Ji W 2007 Optical limiting phenomena of carbon nanoparticles prepared by laser ablation in liquids *J. Phys. Conf. Ser.* **59** 289–92
[32] Chrzanowska J, Hoffman J, Malolepszy A, Mazurkiewicz M, Kowalewski T A, Szymanski Z and Stobinski L 2015 Synthesis of carbon nanotubes by the laser ablation method: effect of laser wavelength *Phys. Status Solidi B-Basic Solid State Phys.* **252** 1860–7
[33] Deshmukh A A, Mhlanga S D and Coville N J 2010 Carbon spheres *Materials Science and Engineering: R: Reports* **70** 1–28
[34] Nieto-Márquez A, Romero R, Romero A and Valverde J L 2011 Carbon nanospheres: synthesis, physicochemical properties and applications *J. Mater. Chem.* **21** 1664–72
[35] Johra F T, Lee J-W and Jung W-G 2014 Facile and safe graphene preparation on solution based platform *J. Ind. Eng. Chem.* **20** 2883–7
[36] Graphene Factory, ACS Material Store 2019 Advance chemicals supplier material https://www.acsmaterial.com/single-layer-graphene-graphene-factory-1049.html
[37] Kartick B, Srivastava S K and Srivastava A I 2013 Green synthesis of graphene *J. Nanosci. Nanotechnol.* **13** 4320–4
[38] Yogesh G K, Shuaib E and Sastikumar D 2017 Photoluminescence properties of carbon nanoparticles synthesized from activated carbon powder (4% ash) by laser ablation in solution *Mater. Res. Bull.* **91** 220–6
[39] Eda G, Lin Y Y, Mattevi C, Yamaguchi H, Chen H A, Chen I S, Chen C W and Chhowalla M 2010 Blue photoluminescence from chemically derived graphene oxide *Adv. Mater.* **22** 505–9
[40] Dorranian D, Solati E and Dejam L 2012 Photoluminescence of ZnO nanoparticles generated by laser ablation in deionized water *Appl. Phys. A-Mater. Sci. Process.* **109** 307–14
[41] Novoselov K S, Geim A K, Morozov S V, Jiang D, Zhang Y, Dubonos S V, Grigorieva I V and Firsov A A 2004 Electric field effect in atomically thin carbon films *Science* **306** 666–9
[42] Nguyen V, Yan L, Si J and Hou X 2015 Femtosecond laser-induced size reduction of carbon nanodots in solution: effect of laser fluence, spot size, and irradiation time *J. Appl. Phys.* **117** 1–6

[43] Haider M J and Mehdi M S 2014 Study of morphology and Zeta potential analyzer for silver nanoparticles *International Journal of Scientific and Engineering Research* **5** 381–5
[44] McNeil S E 2011 *Characterization of Nanoparticles Intended for Drug Delivery* 697 (Berlin: Springer) https://link.springer.com/content/pdf/10.1007/978-1-4939-7352-1.pdf